PROTO-SPHERA, without toroidal magnets, produces and confines plasma tori inside magnetostatic fields

FSN Department, CR-ENEA Frascati

Franco Alladio, Paolo Micozzi, Alessandro Mancuso[retired], Vincenzo Zanza[retired], Fabrizio Andreoli, Gerarda Apruzzese, Luca Boncagni, Paolo Buratti, Fabio Crescenzi, Ocleto D'Arcangelo, Edmondo Giovannozzi, Luigi Andrea Grosso, Alessandro Lampasi, Violeta Lazic, Simone Magagnino, Valerio Piergotti, Mario Pillon, Selanna Roccella, Giuliano Rocchi, Alessandro Sibio, Benedetto Tilia, Angelo Tuccillo, Onofrio Tudisco

FSN Department, CREATE Consortium and retired from CR-ENEA Frascati

Giuseppe Maffia

FSN Department, CREATE Consortium, Physics Department Università Roma-1, la Sapienza

Brunello Tirozzi

PlasmaTech Spin-off of Pisa University and Pisa University

Francesco Giammanco, Paolo Marsili

Pisa University

Danilo Giulietti

Università di Padova e Consorzio RFX and FSN Department, CR-ENEA Frascati

Giuseppe Galatola Teka, Matteo Iafrati

Nature Physics (2018)

Abstract

The PROTO-SPHERA experiment has produced and sustained up to ½ sec axisymmetric magnetically confined current carrying tori around its plasma centerpost discharge. The centerpost discharge is driven by a DC voltage applied between electrodes (DC helicity injection) and the tori are formed in presence of a pre-existing axisymmetric magnetostatic poloidal field only and in absence of any toroidal magnet. This result provides the first hints that future Fusion machines could be built with permanent magnets only.

Main

The use of permanent magnets in toroidal plasma confinement would be a simplification for future controlled fusion reactors. It would avoid any dissipation connected with normal conducting field coils and would have great advantages with respect to superconducting coils, which also remove the ohmic dissipation but require sophisticated cryogenic systems. Magnetic confinement systems based on permanent magnets have never been considered so far, for two reasons: 1) For axisymmetric magnetic confinement[1,2], variable currents are needed for breaking-down the plasma, sustaining its toroidal current and counteracting abrupt plasma displacements, that can trigger MHD instabilities[3]. In non-axisymmetric Stellarators[4] no variable field is needed. However another reason was even more compelling: 2) a toroidal field magnet (irrespective of its axisymmetry) cannot be built with permanent magnets: the single-valued magnetic scalar potential that describes any magnetostatic field outside permanent magnets would be many-valued in the doubly connected domain inside a toroidal field magnet, this implies the necessity of a net poloidal current through the torus hole. This picture could be changed by the results recently obtained in the PROTO-SPHERA experiment[5], where a confined plasma torus, carrying a net toroidal current, has been formed and maintained in absence of any kind of toroidal magnet and in a pre-existing axisymmetric static magnetic field, which fills a simply connected region; in this region such a field is equivalent to a single-valued magnetostatic scalar potential, which could have been produced by permanent magnets. The results found in PROTO-SPHERA have been obtained by normal conducting poloidal field (PF) coils only, so this

paper does not yet deal with the design of a configuration based on axisymmetric permanent magnets.

One of the appealing features of future simply connected axisymmetric magnetic confinement fusion reactors (mirror symmetric with respect to their equator as well) is that they will be endowed, on their symmetry axis and at their edges, with two degenerate X-points[6] (null or neutral magnetic field points). Such fusion reactors could become Fusion Space Thrusters, expelling charged fusion products preferentially from one of the degenerate X-points, acting as a "plasma-nozzle"[7]. In the deep space environment the use of permanent magnets for fusion reactors is the most reasonable possibility, as superconducting magnets would imply the maintenance and the servicing of a cryogenic system, an endeavor that would be very impractical to implement in deep space, if not outright impossible.

The PROTO-SPHERA experiment was recently built in its Phase-1 version[8,9] in the ENEA-Frascati Research Center (Fig.1a). Its purpose is to form a Spherical-Torus (ST, with closed flux surfaces) not around a metal centerpost, as in Tokamaks, but around a Plasma-Centerpost (PC, with open field and fed by electrodes), which is an arc discharge with the magnetic structure of a linear screw pinch, i.e. has both an azimuthal (toroidal) and a longitudinal (poloidal) field component. The original idea was that of getting rid of all the central metal components (toroidal field coils and ohmic transformer), which are the most critical in a Spherical-Tokamak. Thin copper bars outside the vacuum vessel return the Plasma-Centerpost current from a lower collecting ring to an upper ring: they are the only components reminiscent of the outer part of a toroidal magnet in a Tokamak (Fig.1b). Therefore PROTO-SPHERA is a simply connected magnetic configuration: in Phase-2 it will be composed

Fig.1: The general layout of the experiment.

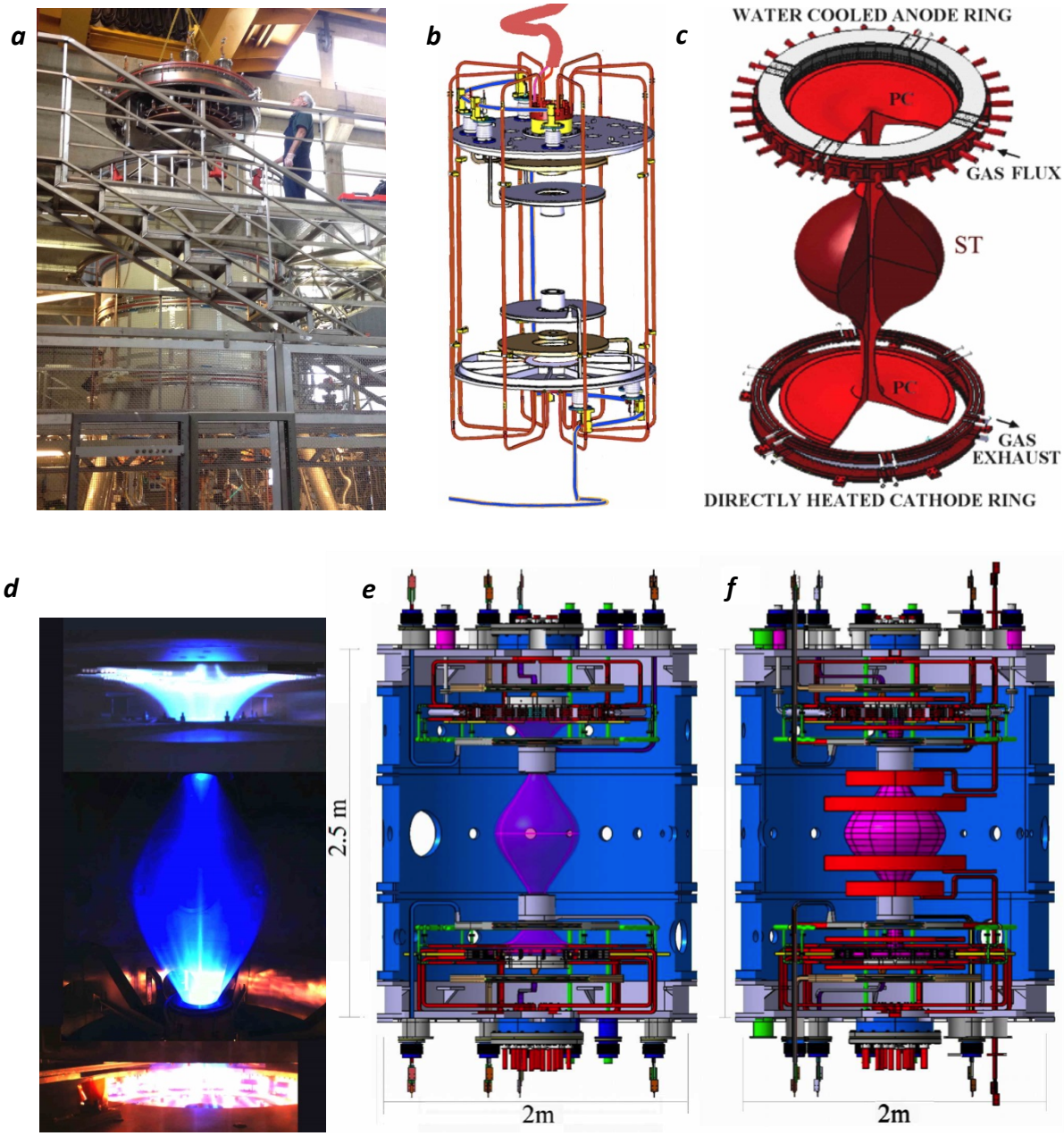

a, The PROTO-SPHERA load assembly (year 2015). b, The copper bars (shown in red) outside the vacuum vessel[10], return the Plasma-Centerpost current from a lower collecting ring to an upper outer coaxial ring; the coaxial cable that feeds the Phase-1 Group-B-PFInt coils is shown in blue. c, Scheme of Spherical-Torus (dark red) around the Plasma-Centerpost (bright red), which terminates on annular electrodes. d, PROTO-SPHERA Argon Plasma Centerpost discharge: pictures from 4 cameras (at different azimuthal angles) are superposed. e, Inside view of the Phase-1 load assembly. f, Inside view of the Phase-2 load assembly.

by a Spherical-Torus (with equatorial diameter $2R_{sph}$=0.7 m and a toroidal plasma current[10] I_{ST}=¼ MA) and by a Plasma-Centerpost (with total length L_{Pinch}≈2 m and midplane diameter ≈0.08 m), fed by annular electrodes (with radius =0.40 m and height =0.04 m), and carrying a longitudinal current I_e=60 kA (electrode plasma current). The Plasma-Centerpost takes the shape of a mushroom in front of both annular electrodes (Fig.1c). However the present Phase-1 of the experiment is a partial set-up of the final machine, built for obtaining the Plasma-Centerpost discharge only (Fig.1d). The vacuum vessel[11] contains only the 8 internal poloidal field of the Group-B-PFInt shaping coils (Fig.1e): they are all connected in series and fed by a unique power supply. To complete the machine a further group (Group-A-PFint, also connected in series) of 10 poloidal field compressing coils will be built (Fig.1f), the 4 largest among them will provide the vertical field required to contain the I_{ST} =¼ MA Spherical-Torus of Phase-2.

The Phase-1 cathode (Fig.2a) is directly heated (Fig.2b), but is only partially filled (Fig.2b) with doubly wound Tungsten-VM (WVM) filament modules[5,12] (Fig.2c): 54 in Phase-1 vs. the 324 that will fill the cathode in Phase-2. The anode[5,12] is a gas-puffed hollow annular anode (Fig.2d) whose plasma facing material is Copper-Tungsten (W-Cu, with 90% W); from its rear the gas discharge is puffed into many hundreds holes facing the plasma, which is then able to enter inside these holes (Fig.2e). On top of the anode plasma it has been already possible to observe the "plasma-nozzle"[7] from the degenerate X-point (Fig.2f).

To obtain the Plasma-Centerpost one has to heat the Tungsten filaments (starting ~30 sec before the plasma); when they have reached ~2900 °C the Group-B-PFInt coils are energized, the shaping field (Fig.3a) is produced

inside the 4 cm thick Aluminum vessel; within a few tens of ms the Centerpost power supply is fired and the screw pinch plasma is produced.

Fig.2: The cathode and the anode of PROTO-SPHERA.

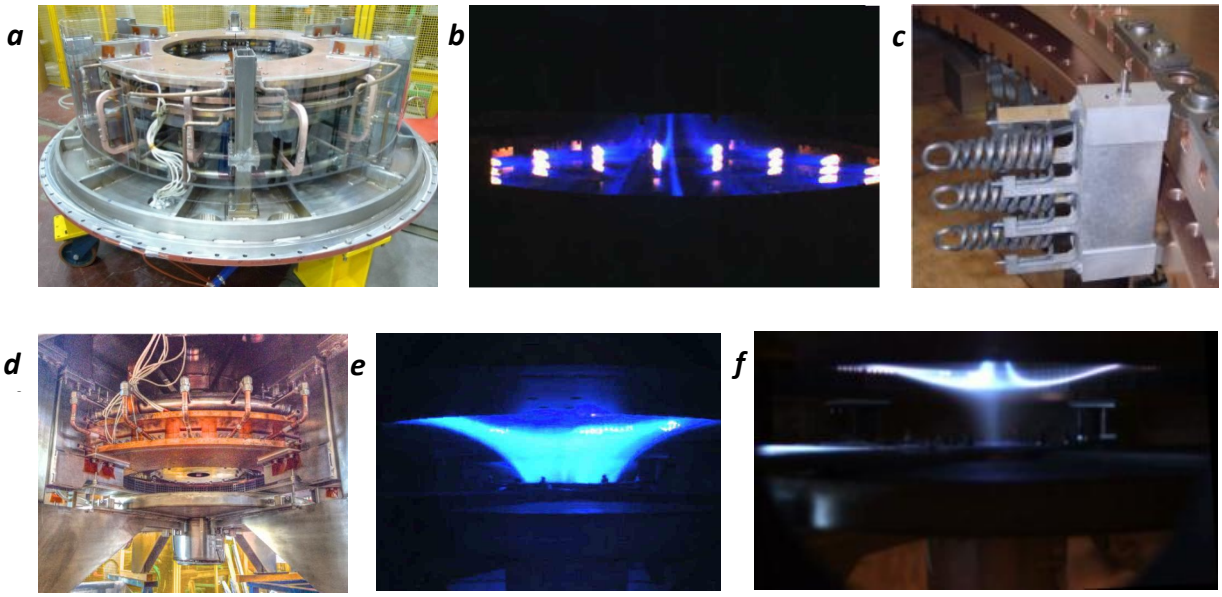

a, The annular cathode resting on the bottom lid. b, Image from the cathode camera during the Argon shot #842: plasma tubes originate from individual Tungsten filaments at ~2900 °C. c, Single module of three Tungsten filaments inserted into the Copper body of the cathode. d, The annular cathode hanging from the top lid. e, Image from the anode camera during Argon shot #954. f, View of the "plasma nozzle"[7] from the upper degenerate X-point on top of the anodic plasma, taken while the Plasma-Centerpost is being switched off.

Two gases were used: Argon and Hydrogen. The 10 kA Plasma-Centerpost in Ar (Fig.3b) was obtained in January 2018, with break-down voltage ~90 V; the electrode plasma current I_e was sustained at 10 kA while the anode-to-cathode voltage increased to ~200 V. The equatorial diameter of the Ar Plasma-Centerpost was $2R_{sph}$~50 cm.

Fig.3: The Plasma-Centerpost produced in Phase-1.

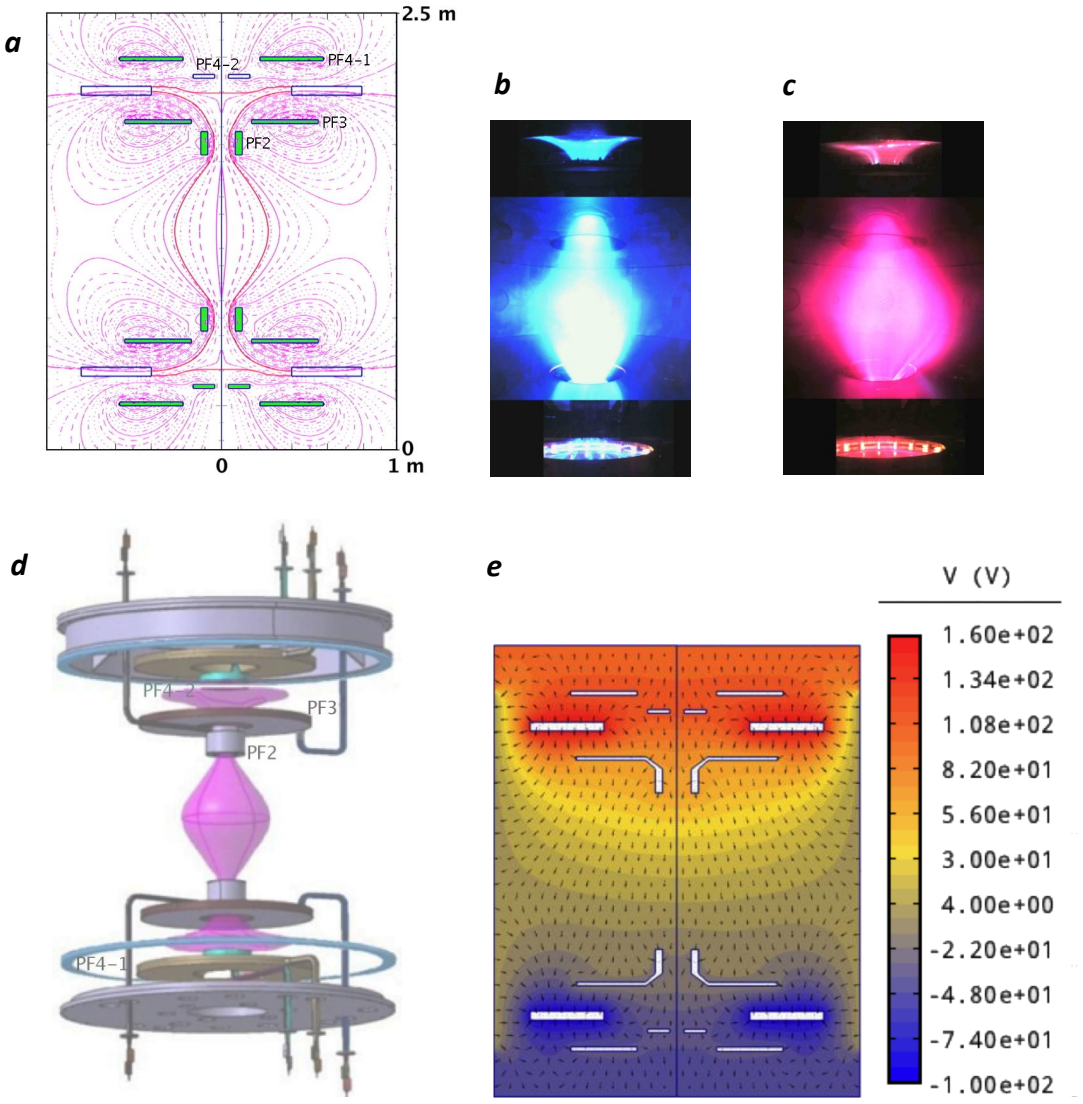

a, Shaping magnetic field produced by the eight Group-B-PFInt coils, the four upper coils are denominated in this figures, the lower four ones being mirror symmetric across the equatorial plane. b, Argon centerpost discharge #954 at I_e=8.5 kA: pictures from 3 cameras (at different azimuthal angles) are superposed. c, Hydrogen discharge #969 at I_e=8.5 kA. d, Inside view of the Phase-1 experiment: the Plasma-Centerpost is drawn in pink color; the Aluminum START[11] cylindrical vessel, the lower AISI304 ferrule and the electrodes are removed: two polycarbonate insulators separate the Aluminum vessel from the two ferrules on top and bottom. b, The electrostatic potential[13] in H discharges at I_e=10 kA (shown with different colors) is not up/down antisymmetric, i.e. the plasma charges the Group-B-PFInt coils on the anode side with a different pattern of electric potential with respect to the cathode side.

The equatorial line-averaged electron density $<n_e>$ in Argon, surprisingly too high for a 4 mm interferometer[14], was measured by a common-path Second-Harmonic-Interferometer (SHI)[15,16] and exhibited a linear dependence upon the electrode plasma current: $<n_e> \propto I_e$, with $<n_e>=4 \bullet 10^{20}$ m^{-3} at I_e=10 kA. As the magnetic field lines start from and end upon electrodes the Plasma-Centerpost temperature cannot be larger than a few eV: it has been determined only at the edge of the anodic mushroom-shaped plasma by Langmuir probe measurements: the local electron temperature was measured to vary from 2 to 8 eV, while the local electron plasma density varied from $n_e=5 \bullet 10^{19}$ m^{-3} to $n_e=2 \bullet 10^{19}$ m^{-3}. Hydrogen too has no interest for Controlled Fusion[17], but it is indicative of the behavior of the Deuterium that will be used in Phase-2 of the experiment. The 10 kA Plasma-Centerpost in H (Fig.3c) was also obtained in January 2018, its break-down voltage was ~320 V and electrode plasma current I_e was sustained at 10 kA while the anode-to-cathode voltage decreased to ~220 V. The equatorial diameter of the H Plasma-Centerpost was $2R_{sph}$~60 cm. The equatorial line-averaged electron density $<n_e>$ of the Hydrogen Plasma-Centerpost was $<n_e>=1.5 \bullet 10^{20}$ m^{-3} at I_e=10 kA. Preliminary results of spectroscopic observations[18] on the plasma equator indicate that in Hydrogen discharges the visible spectrum shows only the Hydrogen lines, whereas the UV spectrum shows limited amounts of metallic impurities. Both Ar and H Plasma-Centerpost discharges were sustained until the anode-to-cathode voltage was applied (1 sec). The much feared anode arc-anchoring of the plasma[19,20] (i.e. the discharge concentrating upon a restricted anode spot, and inflicting local damage) never occurred; the explanation resides in the rotation of the Plasma-Centerpost in the azimuthal (toroidal direction), which is evident from the visible light movies collected by a fast camera. The Plasma-Centerpost

rotates approximately at an angular frequency $\omega=2\pi(5\bullet10^2)$ radians/sec. The cause of such a rotation appears to be the electrostatic charging of the PF coils casings by the plasma itself: all the 8 Group-B-PFInt coils inside the vacuum vessel reach different floating electric potentials (Fig.3d, indicates the names of the Group-B-PFInt coils); also the top part of the vessel (an AISI304 ferrule-and-lid) and its bottom symmetrical ferrule-and-lid are insulated from the grounded Aluminum middle vessel and left floating. In Hydrogen plasma at 10 kA, the anode (top) is charged to +140 V while the cathode (bottom) at -80 V, the top ferrule-and-lid at +95 V while the bottom ferrule-and-lid at -55 V, the two PF4 coils (plasma-nozzle-coils[7]) to +50 V on top and to -10 V on bottom and the PF2\3 coils (mirror-coils) to +95 V on top and -40 V on bottom. Therefore the $E\wedge B$ drift of the plasma, that would be opposite in the anode and cathode region, is not compensated: the top anode has the larger electrostatic field and determines the direction of the net plasma rotation. As the internal magnetic field points upwards, while the electrostatic field goes downwards, from anode to cathode, the net plasma rotation is clockwise (seen from the top of the machine).

The scenario imagined for the production of the Spherical-Torus in Phase-2 of PROTO-SPHERA was to start just like in Phase-1, reaching I_e=8.5 kA for the Plasma-Centerpost current and thereafter to increase rapidly (in ~1 ms) I_e to 60 kA together with the current in the Group-A-PFInt compression coils. Such a current increase would have contained the torus and would have provided at the same time, by induction, a part of its toroidal current: Fig.4a shows the calculated result. Instead in PROTO-SPHERA Phase-1, four external impromptu PFExt coils (Fig.4b) were added and the current in the two PFExt coils nearest to the equatorial plane (Fig.4c) was flown in the

toroidal direction opposite to the one of the toroidal component of plasma current flowing inside the Plasma-Centerpost.

Fig.4: Plasma tori, foreseen for Phase-2 and obtained in Phase-1.

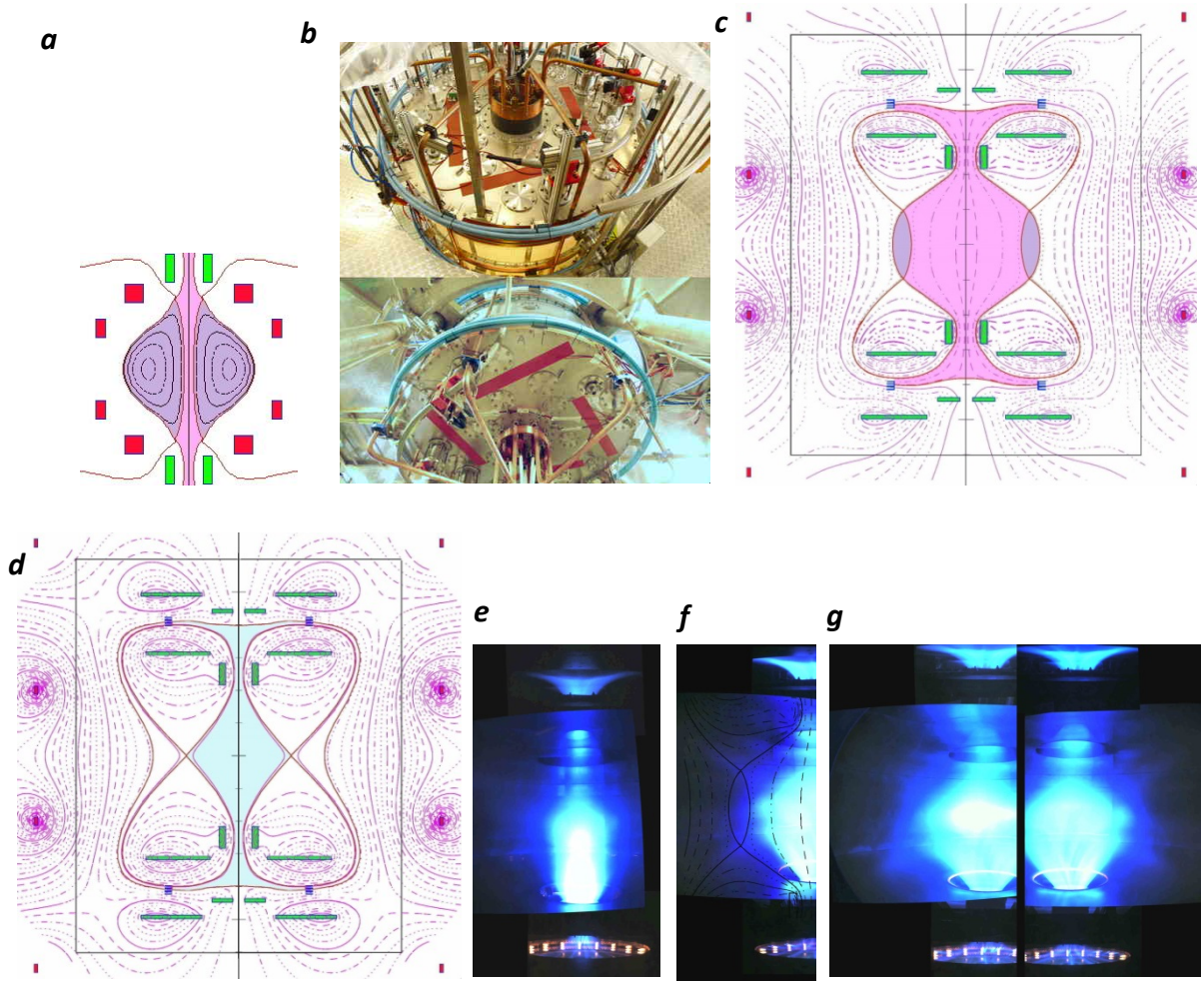

a, Spherical-Torus calculated for the Phase-2 of the experiment, when nearby Group-A-PFInt compression coils (drawn in red) will be added inside the vessel. b, The four additional PFExt coils added outside the vessel (light blue color), viewed from the top and from the bottom lid. c, Calculated equilibrium of a plasma centerpost carrying I_e=10 kA, surrounded by a torus carrying a toroidal current I_{ST} =7 kA, using the four PFExt coils. d, Calculated equilibrium of the Plasma-Centerpost in absence of any torus, but with the PFExt compression coils added outside the vessel. e, Centerpost discharge #1098 in Argon at I_e=3 kA: no torus formation. f, Ar-torus discharge #1160 at I_e=10 kA, superposed with the calculated equilibrium at I_{ST}=5 kA. g, Ar-torus discharges #1149 and #1160 at I_e=10 kA; in the two discharges the fast camera looks at the two opposing sides to show the overall magnetic separatrix.

So that the vertical field could hold in equilibrium a plasma torus, should it form up. The torus formation, because of the outward force due to its toroidal plasma current, would have enlarged the Plasma-Centerpost equatorial outboard, approximately into a portion of sphere. The volume of closed flux surfaces carved out by the torus from the Plasma-Centerpost would have been quite small (<8%): the field of the external PFExt coils in Phase-1 is almost vertical (Fig.4c), whereas the future Group-A-PFInt coils of Phase-2 has been designed in order to carve from the Plasma-Centerpost the largest possible volume of closed flux surfaces (>95%, Fig.4a). The two remaining external PFExt coils (farthest from the equatorial plane) are fed with the opposite direction of current (see Fig.4c), this choice helps in restoring the correct position of the two plasma mushrooms in front of both electrodes, to avoid that they are only partially wetted by the plasma impinging upon them. If the torus was not going to appear, the calculated equilibrium configuration[21] of the Plasma-Centerpost would have had two ordinary X-point (poloidal field $B_{pol}=0$) on the equatorial plane, at ~32 cm from the symmetry axis (Fig.4d), making the Plasma-Centerpost quite narrow. When the electrode plasma current is limited to I_e~3 kA, the plasma indeed conforms to this narrow shape (see Fig.4e). When the current exceeds I_e~8.5 kA, i.e. the (anode-to-cathode) rotational transform of the Plasma-Centerpost overcomes $\iota_e \geq 1/2$ ($q_e \leq 2$ in terms of safety factor), the Ar Plasma-Centerpost takes instead the shape that the equilibrium calculations[21] predict for the torus formation (Fig.4f) and exhibits an axisymmetric double-null (DN) divertor (Fig.4g): a fit of the distance between the two X-points of the DN divertor indicates a toroidal current $I_{ST}=5$ kA inside the Argon-torus (Fig.4c).

The Argon-tori are sustained until the DC anode-to-cathode voltage is applied; for now this time interval is <0.5 sec, as the external field takes 0.6 s to penetrate the 4 cm thick Aluminum vacuum vessel and consequently the plasma break-down has to be delayed. The tori obtained in PROTO-SPHERA Phase-1, with aspect-ratio A~7.5 and elongation b/a=κ~3.5, have never been produced in a Tokamak: such a high aspect-ratio and elongation[22], in absence of a close-fitting conducting wall, would not be sustainable[23,24]. The plasma break-down voltage increases from 90 V in absence of the torus to 200 V, but the anode-to-cathode voltage at the current flat-top increases only from 200 V to 220 V: then the power that the Ar-torus sustainment requires is at most 200 kW, with respect to the 2.0 MW required by the Plasma-Centerpost. The most surprising asset is the unexpected production of the torus in absence of any magnetic flux variation, i.e. in a totally magnetostatic configuration of the axisymmetric poloidal magnetic field pre-existent to the plasma.

After the formation of the Argon-tori the same endeavor was successfully made with Hydrogen plasmas. The presence of Hydrogen-tori is most evident shortly after the plasma break-down (Fig.5a) or during its ramp-down (Fig.5b). The confined torus appears since the first milliseconds after the plasma break-down (the current I_e reaches its flat-top value in ~6 msec) and disappears at a slower rate than the unconfined Plasma-Centerpost, which is ramped-down in ~3 msec. Fig.5c evidences that the confined current flowing inside the torus has a longer persistence than the current flowing between electrodes: in the last msec the torus becomes kink unstable, as the ratio of its poloidal field (i.e. its toroidal confined current) with respect to its toroidal field (i.e. the Plasma-Centerpost current) becomes too large.

Fig.5: Hydrogen-tori from plasma break-down to plasma ramp-down.

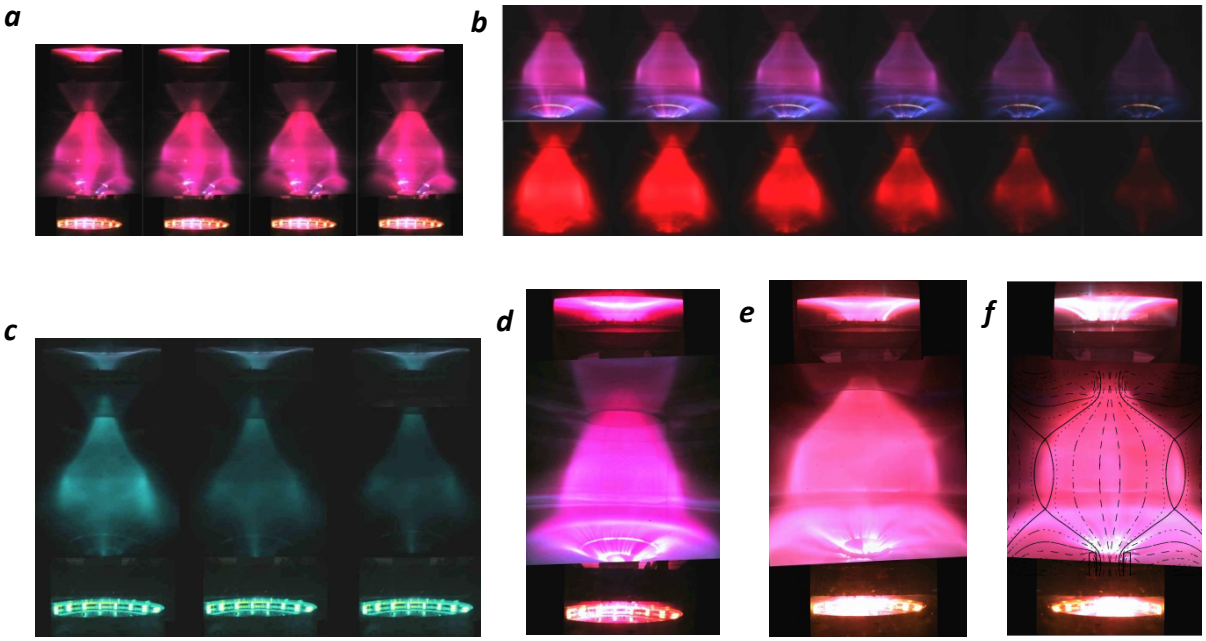

a, Frame sequence (left to right) of torus formation in H discharge #1202, starting 5 ms after plasma break-down (the Plasma-Centerpost current reaches I_e=10 kA in 6 ms), the images of the equatorial fast camera (1/3 ms time resolution) are separated by 1 ms, but the images of the two anode and cathode slow cameras do not change, as their time resolution is 11 ms. b, Top: Sequence of visible light images, during termination of H discharge #1224 which ramps down from I_e=10 kA in 3 ms. Bottom: same for H discharge #1219, observed through a H-alpha interferometric filter. c, Final sequence of plasma (last 1 ms), observed through H-alpha interferometric filter, but better shown by cold-warm color involution, discharge #1219; frames separated by 1/3 ms. d, Divertor fan interacting with the lower polycarbonate diaphragm in H discharge #1202. e, Divertor fan interacting with the lower AISI304 divertor plate in H discharge #1280. f, Hydrogen-torus discharge #1280 at I_e=10 kA at a later time, superposed with the calculated equilibrium at I_{ST}=7 kA.

The tori are limited by a magnetic separatrix endowed with 2 conical divertor fans. Already in Argon the lower (cathodic) divertor fan is dominant (see Fig.4g), the Hydrogen divertor has an even more dominant cathodic fan: almost a single-null (SN) divertor (Fig.5d); the lower divertor fan interacts with the lower polycarbonate diaphragm, which was not deemed to serve as a divertor target. An AISI304 lower divertor plate has been recently inserted

inside the machine, obtaining an improvement in the up/down symmetry of the divertor (Fig.5e) and allowing for a fit[21] of the distance between the two X-points, which indicates a toroidal current I_{ST}=7 kA inside the Hydrogen-torus (Fig.5f). However the lower (cathodic) divertor fan still causes spurious plasma current paths: from the lower divertor, to the plate and finally to the cathode, but through local plasma sparks impinging upon the lower PF2 coil. These parasitic current paths will be removed closing all open spaces between the PF2 and the PF3 coils on bottom ad on top of the machine.

The obtained H-tori have an aspect-ratio A~7 and an elongation b/a=κ~3.5. The vertical field required by Argon-Tori, in terms of the current flowing in the PFext coils (fed in series with the Group-B-PFInt coils), was 12.5% smaller than the maximum current that the PFInt power supply could deliver. Instead for Hydrogen-tori the vertical field requires a current 25% larger than the maximum that the PFInt power supply can deliver. The missing PFExt current was supplemented by adding up a new Supercapacitors[25] based power supply, able to feed a few extra turns of the two PFExt nearest to the equator.

The ratio 1.25/0.875~1.43, between the vertical field required by Hydrogen-tori and the one required by Argon-tori, confirms that I_{ST}~7 kA in H, if I_{ST}~5 kA in Ar. The plasma break-down voltage increases from 320 V (in absence of torus) to 360 V, but the anode-to-cathode voltage at the current flat-top increases only from 220 to 240-255 V: then the power that the H-torus sustainment requires is at most 200-350 kW, with respect to the 2.2 MW required by the H Plasma-Centerpost. However it has to be remarked that this power exceeds what is required for the sustainment of H-tori, being presumably also due to the dissipation of spurious current paths in the lower divertor fan. The robustness of the Plasma-Centerpost+Torus configuration of PROTO-SPHERA is evident, as a disruption never happens: the tori are vertically displaced but survive all the changes of the overall plasma equilibrium, caused by the spurious current paths in the lower Plasma-

Centerpost. The Hydrogen-tori will anyway be sustained for only ¼ sec (see Fig.6a), until their interaction with the divertor plate will not be fully cured.

If the vertical field is in slight excess of the optimal value, say +10%, the Plasma-Centerpost produces odd configurations like Double-Tori and Lop-sided-Tori, all with visible helical components, however also in this case the plasma never disrupts. Instead there are cases where, after a reduced current plasma start-up, with I_e<5 kA for quite long times (up to 0.15 sec), the Plasma-Centerpost current finally achieves I_e=10 kA and forms a proper Plasma-Centerpost+Torus configuration; which is thereafter maintained until the anode-to-cathode DC voltage is applied. Fig.6b illustrates shot #1219, with total duration of ¼ sec, where the plasma remains in a star-shaped state with I_e<5 kA for ~70 ms (first 4 time slices), later increases to I_e=8 kA in a Double-Torus configuration and finally metamorphoses (last 100 ms) into a proper Plasma-Centerpost+Torus configuration. This initial difficulty to form a torus suggests that the plasma discharge has a part where the current flows in the Plasma-Centerpost but the rest of the plasma discharge seems trapped in a axisymmetric-toroidal-cusp configuration[26,27] (Fig.6c), coherent with the hexapolar character of the poloidal field pre-existent to the plasma (Fig.6d).

Also the poloidal field required for PROTO-SPHERA in Phase-2, for shaping and compressing the Spherical-Torus at I_{ST}=¼ MA, has an hexapolar character, with the complication that the two electrodes (see Fig.6e) are magnetically disconnected from each other. This disconnection implies possible difficulties in setting up a Plasma-Centerpost current in a purely static poloidal field pre-existent to the plasma. Therefore it seems possible that PROTO-SPHERA in Phase-2 will really have to form up increasing both the Plasma-Centerpost current I_e to 60 kA as well as the current in the Group-A-PFInt compression coils, but on a slow time scale, of a few tens of msec. Such a slow rise however opens the attractive possibility of a feedback-controlled Spherical-Torus formation.

Fig.6: Torus sustained ¼ s & metamorphosis of a toroidal cusp into a torus.

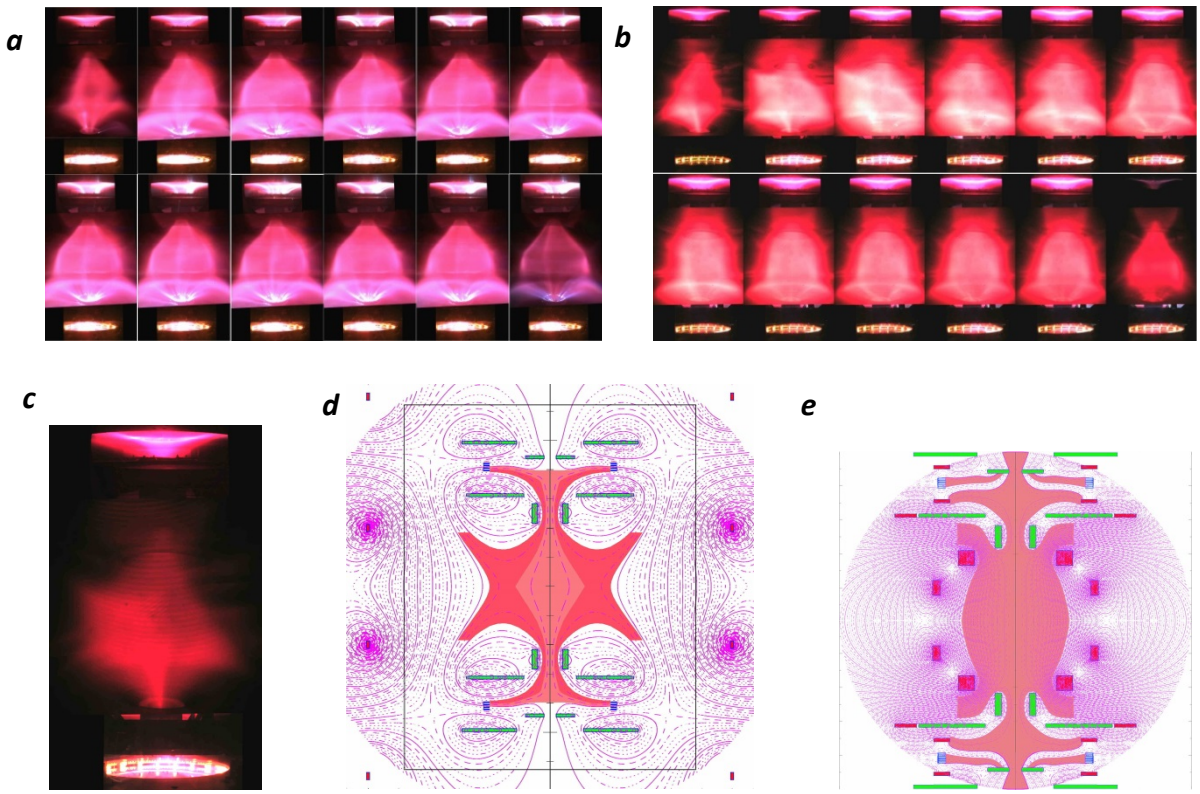

a, Frame sequence (left to right and top to bottom) of equally time-spaced, visible light pictures of H-torus sustainment in discharge #1280, lasting 0.25 sec, with I_e=10 kA and with AISI304 lower divertor plate. b, Same for H-alpha filtered images of the H-torus discharge #1219, with polycarbonate lower divertor plate. In the first 3 frames I_e does not overcome 5 kA and there is no torus, later I_e reaches 10 kA and the configuration metamorphoses into a torus. c, Hexapolar toroidal cusp configuration, in the initial H shot #1221. d, The hexapolar character of the poloidal field pre-existent to the plasma break-down in those two shots. e, The hexapolar character of the poloidal field able to contain the ¼ MA Spherical-Torus of PROTO-SPHERA calculated for Phase-2: the two electrodes (blue) become disconnected from each other, in terms of the pre-existing axisymmetric configuration of static poloidal field.

The evidence that the Hydrogen-tori can appear since the first milliseconds after the plasma break-down in perfectly static field conditions rules out any interpretation in terms of inductive phenomena. The only induction being the one associated with the current increase in the Plasma-Centerpost itself, just after the break-down: a loop voltage of less than 0.1 V for a few ms would

drive a current in a direction opposite to the current winding around the Plasma-Centerpost; such reverse direction current in the torus could not be held in equilibrium by the external PFExt coils. The field imposed by the Group-B-PFInt coils is going upwards near the symmetry axis, whereas the current density is going downwards from anode to cathode, so in the Plasma-Centerpost the sign of $\vec{j}\bullet\vec{B}$ is negative and the plasma current winds in the Centerpost in the anticlockwise direction (seen from above). Also the current in the torus is anticlockwise, as the current in the PFExt is in the clockwise direction and confines the torus. Then the sign of the toroidal current in the torus is the same as the sign of the toroidal current in the Plasma-Centerpost: the sign of $\vec{j}\bullet\vec{B}$ is negative all over the plasma[28,29]. This is a clear sign that it is a DC Helicity Injection in charge of transferring plasma current from the centerpost to the torus, just as it was imagined when the PROTO-SPHERA experiment was designed. The presence of ordinary X-points in the DN divertor is a second hint that magnetic reconnections are responsible for the sustainment of the torus: in the 2D approximation magnetic reconnections occur naturally at ordinary X-points[30], albeit 3D effects[31] are present, as indicated from the diffused (ergodic) character of the X-points observed in PROTO-SPHERA. The third hint to magnetic reconnection is, for Hydrogen-tori, the repetition of distinctive bursts that shake the plasma shape, with an irregular quasi-periodicity of 2-3 msec; such bursts are accompanied by emissions of plasma into the separatrix fans. These occurrences are quite reminiscent of the bursting nature of the “Flux Transfer Events” in the Earth Magnetosphere[32] and of “Solar Flare X-Ray Emission”[33], not to mention the repetitive, but not fully periodic, occurrence of “Sawtooth Oscillations” [34,35] and of “ELM’s activity”[36,37] in Tokamaks.

The results illustrated in this paper deal with the first production of plasma tori in the PROTO-SPHERA experiment, they indicate that:

1) There is no unavoidable need of a toroidal magnet for producing quasi-axisymmetric magnetically confined tori: a Plasma-Centerpost discharge, sustained by DC voltage between two electrodes, is sufficient for obtaining such an aim.
2) The tori can be produced in a pre-existing axisymmetric configuration of magnetostatic poloidal field: no variations are required in the poloidal fields that (as per the virial theorem) surround and contain the plasma.
3) The magnetically confined tori can be maintained in quasi-steady state, i.e. until the anode-to-cathode DC voltage is applied: magnetic reconnections are able to provide a completely steady-state current drive to the toroidal plasma.
4) No disruption phenomena occur in the PROTO-SPHERA magnetic confinement configuration. The Plasma-Centerpost+Torus configuration can even produce tori (like the ones here illustrated) that have an aspect ratio A=7 with an elongation κ=3.5, which in a Tokamak could absolutely not be produced and sustained.

After many decades, during which magnetic reconnections were the nightmare of magnetic containment schemes, a useful application of these natural plasma phenomena could have appeared in magnetic confinement, hopefully to be consolidated by more significant plasma discharges in future experimental rounds and, if possible, to be further extended to obtain from them a vigorous and self-organized plasma heating[38,39,40] for the Phase-2 of PROTO-SPHERA, where a total power of ~15 MW is expected to be input into

the overall plasma. Phase-2 of the experiment will assess the full potential of this new configuration, when the closed flux surfaces volume that the torus carves out from the spherically shaped Plasma-Centerpost will increase from <8% to >95%. If the properties observed in Phase-1 will remain valid and furthermore if the energy confinement time will be long enough, this configuration may even be able to solve many issues that have remained unsolved in the Tokamak case: the removal of the disruption problem and the necessity of powerful plasma heating and current drive that, instead of requiring complicated external systems, will become embedded into the magnetic configuration itself and will rely upon the spontaneous natural phenomenon of magnetic reconnections.

All these points, when put together, give an even stronger conclusion: magnetic confinement devices to study Controlled Fusion could in principle be built using axisymmetric permanent magnets only, able to provide a poloidal magnetostatic field pre-existent to the plasma. A Plasma-Centerpost fed by electrodes will produce and sustain the confined torus in such a poloidal field. In case the two electrodes become disconnected from each other, in terms of the pre-imposed axisymmetric configuration of permanent magnets poloidal field, currents of short duration, flowing in a few simply conducting coils, could be required in addition to the permanent magnets: however the currents of these coils would be gradually switched off after the plasma break-down and would vanish when the proper final confinement configuration, to be sustained by permanent magnets only, is achieved.

Methods

Load assembly and power supplies

The PROTO-SPHERA load assembly was built in the years 2007-2009 by ASG Superconductors in Genova (Italy) inside the 2 m diameter START vacuum vessel[11], kindly gifted by the Euratom-UKAEA British Association.

The Group-B-PFInt coils are fed by a DC machine that delivers 2 kA at 350 V DC, built by EEI in Vicenza (Italy), in the years 2011-2014. A further power supply for the new Group-A-PFInt compression coils will be built in Phase-2, as a DC machine able to deliver 1.2 kA at 600 V to the 10 new coils connected in series.

The Plasma Centerpost power supply, built by EEI as well, is instead limited to the first unit (I_e =10 kA at 350 V DC, for 1.1 sec); a second unit will be built in Phase-2, able to increase the electrode plasma current up to I_e=60 kA.

The electrical power supply for heating up the cathode is a six-phased AC machine, also built by EEI, able to deliver 1.7 kA up to 25 V rms to the nine Tungsten filaments present per phase at this moment; its current capability will be increased to 10 kA per phase in the Phase-2 version, where 54 Tungsten filaments will be present per phase, in order to increase the electrode plasma current up to I_e=60 kA.

A new power supply based upon Supercapacitors[25] (2 kA at 96 V DC for a few sec, with a rise time longer than 20 ms), built by OCEM in Bologna, has been introduced in 2018, able to increase the vertical field produced by the PFExt coils external to the vessel, in order to meet the requirements imposed by the formation of the Hydrogen tori.

With the exception of the six-phased AC Cathode heating power supply all the conductors that carry the currents of the power supply are coaxial cables (see Fig.1b); in particular the Plasma Centerpost power supply is fed through two coaxial metal rings on top of the machine, in order to minimize any error field.

From Fig.3a it is possible to see that an ordinary X-point (poloidal field B_{pol}=0) is present on the equatorial plane inside the vacuum vessel at only ~30 cm from the Aluminum wall. In order to change the magnetic boundary conditions four external additional PFExt coils were added (Fig.4b). However the presence of the 4 cm thick Aluminum vacuum vessel and of the two groups of AISI304 ferrule-and-lid on top and bottom (see Fig.6a) introduces a skin current that opposes the applied external magnetic and that is totally dissipated in the Aluminum only after 0.6 sec. Therefore, in order to achieve steady state conditions with the combined (internal+external) shaping field, the break-down of the plasma must be delayed by ~0.6 sec: the maximum duration of the plasma discharge is then reduced from 1.1 sec to just 0.5 sec.

A new insulating vacuum vessel (made out of very thick transparent PMMA, poly-methyl-methacrylate, being built by Reynolds Polymer Technology in Grand Junction, CO, USA) will be installed in 2019, then the problem of the skin current inside the present Aluminum vessel will disappear; four new PFExt external field coils with less resistance will be set up around the PMMA vessel, such that the existing Supercapacitor power supply will be able to feed the whole new PFExt series of coils; it will therefore become possible to test already in Phase-1 an impulsive torus formation with a 20 ms rise time.

Insulation problems

Argon has no interest whatsoever for Controlled Fusion, it was employed only as its break-down voltage is very low, from 2015 to end of 2017 Ar was the gas of choice for learning how to cure a number of insulation problems: a 2 mm thick polycarbonate foil lines the inside of the Aluminum vessel and two 1 cm thick polycarbonate diaphragms have been glued to this foil near the two PF2 “mirror coils” (Fig.3a contains all the PF coils names): the translucent polycarbonate disturbs the images collected by a fast wide-angle videocamera looking at the Plasma Centerpost, because multiple reflections can occur.

Both upper and lower parts are separated from the electrically grounded Aluminum cylinder by two 1 cm thick insulating Polycarbonate rings (see Fig.3a): the total height of the PROTO-SPHERA vessel is therefore extended (with respect to START[11], which was originally 2 m tall) by the two ferrules and reaches 2.52 m.

Magnetic measurements

A large number of magnetic probes (about 70) are present near the anode and near the cathode plasma regions, but there are not magnetic measurements near the torus (in Phase-1 no magnetic probes were integrated in the main chamber between the two PF2 “mirror coils”, as the formation of a torus was not foreseen) however the distance between the two X-points[21] of the DN divertor gives an accurate estimate of the current flowing inside the torus.

The measurements of the original Rogowsky coils that measure the Plasma Centerpost currents that go through the two PF2 “mirror coils” (see Fig.3a) have been doubly checked by two supplementary Rogowsky coils that have been built from the armored cable kindly offered by the firm Axon Cable of

Montmirail (France) and inserted inside the machine just before attempting the formation of the plasma torus.

Plasma diagnostics

Initial attempts of measuring the Ar Plasma Centerpost equatorial line-averaged electron density $<n_e>$ by a 4 mm interferometer[14] were unsuccessful, because the density was higher than expected but they gave anyhow an interesting information: although the 4 mm microwave beam was in cutoff no reflected signal was observed, hinting to the existence of a significant gradient of electron density from bottom (larger) to top of the Plasma Centerpost (smaller), able to deflect the microwave beam in the vertical direction; also the visible images of Ar discharges (Fig. 2a and 3a) show a relevant vertical inhomogeneity of the light emission.

The line-averaged electron density $<n_e>$ of the Ar Centerpost has been therefore measured on the equatorial plane, by a common-path Second Harmonic Interferometer (SHI)[15,16]. The SHI, developed by the "Plasma Diagnostics & Technologies SRL" (a spin-off of the University of Pisa), is a device insensitive-to-vibrations, which has allowed an easy installation on the machine, thanks to a compact modular design. In Hydrogen discharges, electrode plasma currents much lower than 10 kA exhibited large variation and were rather difficult to be maintained with steady currents, so the only reliable line-averaged electron density measurements were performed at I_e=10 kA, where the equatorial line-averaged electron density was $<n_e>=1.5\bullet10^{20}$ m^{-3}.

Optical emission (OE) from the Proto-Sphera device is detected by a compact spectrometer array[18] covering the range 235-790 nm, with the resolution from 0.09 nm in UV to 0.14 nm in IR.

The fast camera that records the largest central portion of the plasma in visible light, or with an interferometric H-alpha filter in front of the CCD, has full images of 1024•1024 pixels and sampling rate of ~3kHz.

A radiation survey monitor has been used to verify the presence of hard x-rays radiation emission during the formation of the plasma arc and torus configuration. The monitor used was a Victoreen gamma x ray ionization chamber with an energy measuring range from about 20 keV up to 3 MeV. The integral of the total dose was measured during some pulses in a position near a glass window facing the plasma equator but signals above the background were never detected. This is consistent with the high density of the plasma produced by PROTO-SPHERA.

References

1 J. Wesson, *Tokamaks,4th ed.*, Oxford University Press, Oxford (2011)

2 D.H. Crandall, , C.W. Hartman, Y.K.M. Peng, A.L. Hoffman, R.A. Krakowski, J.D. Sethian, A.E. Robson, Reversed field pinch, Compact Toroids, and Dense Z-pinch, *J Fusion Energy* **8**, 9–25 (1989)

3 J. Manickam, Allen H. Boozer, and Stefan Gerhardt, Kink modes and surface currents associated with vertical displacement events, *Phys. Plasmas* **19**, 082103 (2012)

4 Allen H. Boozer, What is a stellarator?, *Physics of Plasmas* **5**, 1647 (1998)

5 F. Alladio, A. Mancuso, P. Micozzi, L. Pieroni, C. Alessandrini, G. Apruzzese, L. Bettinali, P. Buratti, A. Coletti, P. Costa, C. Crescenzi, A. Cucchiaro, R. De Angelis, T. Fortunato, D. Frigione, M. Gasparotto, G. Gatti, R. Giovagnoli, L.A. Grosso, G. Maddaluno, G. Maffia, S. Mantovani, G. Monari, C. Nardi, S. Papastergiou, M. Pillon, A. Pizzuto, M. Roccella, F. Rogier, M. Santinelli, L. Semeraro, A. Sibio, B. Tilia, O. Tudisco, L. Zannelli, V. Zanza, PROTO-SPHERA, ENEA, Serie Energia, Associazione Euratom-ENEA sulla Fusione, RT/ERG/FUS/2001/14, ISSN: 1124-7932 (2001)

6 M. Tuszewski, Field Reversed Configurations, *Nucl. Fusion* **28**, 2033 (1988)

7 F. Rogier, G. Bracco, A. Mancuso, P. Micozzi, and F. Alladio, Simply Connected High-Beta Magnetic Configurations, *11TH INTERNATIONAL CONGRESS ON PLASMA PHYSICS: ICPP 2002*, *AIP Conference Proceedings* **669**, 557 (2003)

8 F. Alladio, P. Costa, A. Mancuso, P. Micozzi, S. Papastergiou and F. Rogier, Design of the PROTO-SPHERA experiment and of its first step (MULTI-PINCH), *Nucl. Fusion* **46**, S613–S624 (2006)

9 A. Lampasi, G. Maffia, F. Alladio, L. Boncagni, F. Causa, E. Giovannozzi, L.A. Grosso, A. Mancuso, P. Micozzi, V. Piergotti, G. Rocchi, A. Sibio, B. Tilia and V. Zanza, Progress of the Plasma Centerpost for the PROTO-SPHERA Spherical Tokamak, *Energies***9**(7), 508 (2016)

10 P. Micozzi, F. Alladio, A. Mancuso and F. Rogier, Ideal MHD stability limits of the PROTO-SPHERA configuration, *Nucl. Fusion* **50**, 1-10 (2010)

11 A. Sykes, E. Del Bosco, R.J. Colchin, G. Cunningham, R. Duck, T. Edlington, D.H.J. Goodall, M.P. Gryaznevich, J. Holt, J. Hugill, J. Li, S.J. Manhood, B.J. Parham, D.C. Robinson, T.N. Todd and M.F. Turner, First results from the START experiment, *Nucl. Fusion* **32**, 694 (1992)

12 F. Alladio, L.A. Grosso, A. Mancuso, S. Mantovani, P. Micozzi, G. Apruzzese, L. Bettinali, P. Buratti, R. De Angelis, G. Gatti, G. Monari, M. Pillon, A. Sibio, B. Tilia, O. Tudisco, Results of Proto-Pinch Testbench for the PROTO-SPHERA experiment, *Proc. of the 27th EPS Conference on Contr. Fusion and Plasma Phys. Budapest, 12-16 June 2000*, ECA Vol. 24B, 161-164 (2000)

13 Karban, P., Mach, F., Kůs, P., Pánek, D., Doležel, I., Numerical solution of coupled problems using code Agros2D, *Computing* **95** Issue 1 Supplement, 381-408 (2013)

14 O. Tudisco, A. Lucca Fabris, C. Falcetta, L. Accatino, R. De Angelis, M. Manente, F. Ferri, M. Florean, C. Neri, C. Mazzotta, D. Pavarin, F. Pollastrone, G. Rocchi, A. Selmo, L. Tasinato, F. Trezzolani, and A.A. Tuccillo, A microwave interferometer for small and tenuous plasma density measurements, *Review of Scientific Instruments***84**, 033505 (2013)

15 F. Brandi, F. Giammanco, W.S. Harris, T. Roche, E. Trask, and F.J. Wessel, Electron density measurements of a field-reversed configuration plasma using a novel compact ultrastable second-harmonic interferometer, *Review of Scientific Instruments* **80**, 113501 (2009)

16 T. Del Rosso, F. Giammanco, M.G. Anderson, F. Conti, A. Balvis, I. Isakov, V. Matvienko, G. Strashnoy, W. Waggoner, L. Bonelli, E. Paganini, and M.W. Binderbauer, Long-path second-harmonic interferometer with nanosecond time resolution: reliable diagnostic tool for electron density measurement in pulsed plasma devices, *Optics Letters* **37**, No. 18 3855 (2011)

17 H.A. Bethe and C.L. Critchfield, The formation of Deuterons by Proton combination, *Phys. Rev.* **54**, 248 (1938)

18 V. Lazic, A. De Ninno, Calibration approach for extremely variable laser induced plasmas and a strategy to reduce the matrix effect in general, *Spectrochimica Acta Part B* **137**, 28–38 (2017)

19 D.L. Murphree, R.P. Carter, Observations on magnetically induced anodic arc region behavior, *Journal of Applied Physics* **45**, 1915 (1974)

20 H.C. Miller, A review of anode phenomena in vacuum arces, *Contributions to Plasma Physics* **23**, 223-249 (1989)

21 F.Alladio and P. Micozzi, Reconstruction of Spherical Torus Equilibria in Absence of Magnetic Measurements in the Central Cavity, *Nucl. Fusion* **37**, 1759 (1997)

22 S.C. Cowley , P.K. Kaw , R.S. Kelly , and R.M. Kulsrud, An analytic solution of high beta equilibrium in a large aspect ratio tokamak, *Physics of Fluids B* **3** , 2066 (1991)

23 R.D. Stambaugh, L.L. Lao, E.A. Lazarus, Relation of vertical stability and aspect ratio in Tokamaks, *Nucl. Fusion* **32**, 1642-1646 (1992)

24 R. Fitzpatrick, A sharp boundary model for the vertical and kink stability of large aspect-ratio vertically elongated tokamak plasmas, *Physics of Plasmas* **15**, 092502 (2008);

25 G. Maffia, A. Lampasi, and P. Zito, A new generation of pulsed power supplies for experimental physics based on supercapacitors, *IEEE 15th International Conference on Environment and Electrical Engineering (EEEIC)*, 1067-1072 (2015)

26 J.B. Taylor, Some Stable Plasma Equilibria in Combined Mirror-Cusp Fields, *Physics of Fluids* **6**, 1529 (1963)

27 R. Jones, Plasma confinement in an axisymmetric toroidal multipole cusp, *Il Nuovo Cimento B* **78**, pp 249–254 (1983)

28 J.B. Taylor, Relaxation of Toroidal Plasma and Generation of Reverse Magnetic Fields, *Phys. Rev. Lett.* **33**, 1139 (1974)

29 J.B. Taylor and M.F. Turner, Plasma current drive by helicity injection in relaxed states, *Nucl. Fusion* **29**, 219-229 (1989)

30 R.L. Stenzel and W. Gekelman, Magnetic Field Line Reconnection Experiments 1. Field Topologies, *Journal of Geophysical Research* **86**, 649-658, (1981)

31 V.E. Parnell, J.M. Smith, T. Neukirch, and E.R. Priest, The structure of three-dimensional magnetic neutral points, *Phys. Plasmas* **3**, 759-770 (1996)

32 D.J. Southwood, C.J. Farrijgia And M.A. Saunders, What Are Flux Transfer Events?, *Planet. Space Sci.* **36**, 505-508, (1988)

33 P.E. Fehlau, W.H. Chambers, J.C. Fuller, W.E. Kunz, R.W. Milkey And N.K. Blocker, Periodic Solar Flare X-ray Emission, *Nature* **232**, 42–43 (1971)

34 V. Goeler, et al. Studies of internal disruptions and m= 1 oscillations in tokamak discharges with soft–x-ray techniques, *Phys. Rev. Lett.* **20**, 1201 (1974)

35 B.B. Kadomtsev, Disruptive instability in tokamaks, *Soviet Journal of Plasma Physics* **1**, 389-391 (1975)

36 F. Wagner, G. Becker, K. Behringer, D. Campbell, A. Eberhagen, W. Engelhardt, G. Fussmann, 0. Gehre, J. Gernhardt, G.V. Gierke, G. Haas, M. Huang, F. Karger, M. Keilhacker, Q. Kluber, M. Kornherr, K. Lackner, G. Lisitano, G.G. Lister, H.M. Mayer, D. Meisel, E.R. Müller, H. Murmann, H. Niedermeyer, W. Poschenrieder, H. Rapp, H. Bohr, F. Schneider, G. Siller, E. Speth, A. Staebler, K.H. Steuer, G. Venus, O. Vollmer, and Z. Yu., Regime of Improved Confinement and High Beta in Neutral-Beam-Heated Divertor Discharges of the ASDEX Tokamak, *Phys. Rev. Lett.* **49**, 1408-1412 (1982)

37 A. Kirk, H.R. Wilson, R. Akers, N.J. Conway, G.F. Counsell, S.C. Cowley, J. Dowling, B. Dudson, A. Field, F. Lott, B. Lloyd, R. Martin, H. Meyer, M. Price, D. Taylor, M. Walsh and the MAST team, Structure of ELMs in MAST and the implications for energy deposition, *Plasma Phys. Control. Fusion* **47**, 315 (2005)

38 R.L. Stenzel, W. Gekelman, and N. Wild, Magnetic Field Line Reconnection Experiments 4. Resistivity, Heating, and Energy Flow, *Journal of Geophysical Research* **87**, 111-117 (1982)

39 E.G. Zweibel and M. Yamada, Magnetic Reconnection in Astrophysical and Laboratory Plasmas, *Annu. Rev. Astron. Astrophys.* **47**, 291–332 (2009)

40 E.G. Zweibel and M. Yamada, Perspectives on magnetic reconnection, *Proc. R. Soc.* A **472**, 20160479 (2016)